

# GIS Based Realistic Weather Radar Data Visualization Technique

Bong-Joo Jang<sup>1,\*</sup>, Sanghun Lim<sup>2</sup>

## Abstract

In recent years, the quixotic nature and concentration of rainfall due to global climate change has intensified. To monitor localized heavy rainfalls, a reliable disaster monitoring and warning system with advanced remote observation technology and high-precision display is important. In this paper, we propose a GIS-based intuitive and realistic 3D radar data display technique for accurate and detailed weather analysis. The proposed technique performs 3D object modeling of various radar variables along with ray profiles and then displays stereoscopic radar data on detailed geographical locations. Simulation outcomes show that 3D object modeling of weather radar data can be processed in real time and that changes at each moment of rainfall events can be observed three-dimensionally on GIS.

**Key Words:** 3D modeling, GIS, Radar data visualization, Weather radar

## I. INTRODUCTION

In the last decade, with the introduction of Doppler and dual-polarization technology, weather radars have evolved significantly. The accuracy of weather phenomena interpretation has also improved with high spatiotemporal radar observation [1]. Along with these developments in weather radars, radar based severe weather monitoring and forecasting studies have been extensively conducted. Furthermore, national disaster prevention systems and related services have been established. In particular, in regions where loss of life and property damage frequently occur due to severe weather phenomena such as tornados, localized heavy rainfall, and flash floods, the advanced weather radar system plays an important role for real-time weather monitoring and forecasting in an attempt to minimize these damages.

For radar based weather monitoring system, there is growing interest in the real-time mapping of radar observations on the geographical information system (GIS) and the visualization methods of radar data based on spatial interpolation techniques [2-4]. Currently, the method of displaying radar data in the 2D GIS coordinate system has been extensively used for providing weather information from weather radar. However, it is likely that there is a degree of mapping uncertainty because the elevation of the radar beam and other similar factors are

not considered in 2D display methods. Furthermore, mapping to the ground observation from above ground proves difficult. To solve these problems, display systems such as constant altitude plan position indicator (CAPPI) and radar product processing system (PPS), which synthesize radar data observed at various angles of altitude, have been developed[5,6]. However, since scans are done at several altitudes to obtain observations over a volume, mapping accuracy decreases due to time delay and observation time differences during scans. The radar community has also developed techniques to construct 3D volume data by using plan position indicators (PPIs) data at several altitude angles and/or range height indicators (RHIs) data at several azimuths in order to infer the overall size, development, and dissipation of the weather echo[7]. However, such 3D data construction methods have several limitations: real-time work and calculation is complicated. In addition, these methods are not able to show clutter and beam shading region intuitively.

In this paper, we propose a GIS-based high-resolution realistic radar data display method via 3D radar beam radiation modeling. This method can provide users the stereoscopic observation of weather phenomena changes and a way in which to easily discriminate occultation region that occurs from beam blockage. Clutter and shadowing resulted in terrain blockage are especially problematic for radar based quantitative precipitation

---

Manuscript received March 27, 2017; Revised March 31, 2017; Accepted April 09, 2017. (ID No. JMIS-2017-0001)

Corresponding Author (\*): Sanghun Lim, 283 Goyangdae-Ro Ilsanseo-Gu Goyang-Si Gyeonggi-Do 10223 Korea, +82-31-9100-373, [slim@kict.re.kr](mailto:slim@kict.re.kr)

<sup>1</sup>Korea Institute of Civil Engineering and Building Technology, Goyang-Si, Republic of Korea, [roachbjb@kict.re.kr](mailto:roachbjb@kict.re.kr)

<sup>2</sup>Korea Institute of Civil Engineering and Building Technology, Goyang-Si, Republic of Korea, [slim@kict.re.kr](mailto:slim@kict.re.kr)

---

estimation (QPE) and precipitation pattern recognition[8]. Ground clutter can be misinterpreted as heavy precipitation and therefore overestimations of QPE may occur, whereas QPE underestimations may occur at beam occultation areas after terrain blockage. The proposed display technique that adopts GIS and 3D radar beam radiation modeling can provide users exact locations of clutter and shadowing in order to prevent misinterpretation of precipitation rate or patterns.

The paper is organized as follows: section 2 reviews the process of data generated from the weather radar and section 3 describes the proposed technique in detail. Section 4 demonstrates the test results via simulation of the proposed technique. Finally, section 5 summarizes the proposed method and details the advantages

## II. BACKGROUND OF WEATHER RADAR DATA PROCESSING

Lately, the most important technologies in weather radar are dual polarization and networked radar sensing. The X-band radar network has become more popular for urban and mountainous applications with low-level coverage and high spatiotemporal resolution. Single-polarization Doppler radars, which use only one polarization such as horizontal or vertical direction, output the parameters reflectivity ( $Z$ ), Doppler velocity ( $V$ ), and spectrum width ( $W$ ) as part of radar products. Meanwhile, dual-polarization radars, in addition to  $Z$ ,  $V$  and  $W$ , obtain dual-polarization products such as differential reflectivity

( $Z_{dr}$ ), differential propagation phase ( $\Phi_{DP}$ ), copolar correlation coefficient ( $R_{hoHV}$ ), and specific differential phase ( $K_{dp}$ ) [9]. By obtaining such dual-polarization radar variables, precipitation types (rain, snow, hail, etc.), which are difficult to discriminate by using single-polarization radar observations, can be distinguished and the amount of rainfall can be measured more accurately. Figure 1 shows the flow of data processing and data formation of a typical dual-polarization radar. From the process shown in Figure 1(a), the various radar variables mentioned above can be obtained via signal processing and filtering of in-phase and quadrature signals; horizontal polarization signals  $I_h$ ,  $Q_h$  and vertical polarization signals  $I_v$ ,  $Q_v$ , which are obtained from the signals emitted while the radar antenna rotates. Figure 1(b) shows an example of the reflectivity ( $Z$ ) among the 1D radar variables, which is dependent on observation distance, formed in real time through the process shown in Figure 1(a). By performing coordinate change and spatial interpolation of radar variables, which are represented in the 1D ray shown in Figure 1(b), one PPI or one RHI radar image can be constructed over each azimuth or elevation.

## III. PROPOSED 3D RADAR DATA VISUALIZATION

When the radar beam encounters terrain or buildings, propagating radar signal power decreases according to the degree of occultation. Showing the blockage region is

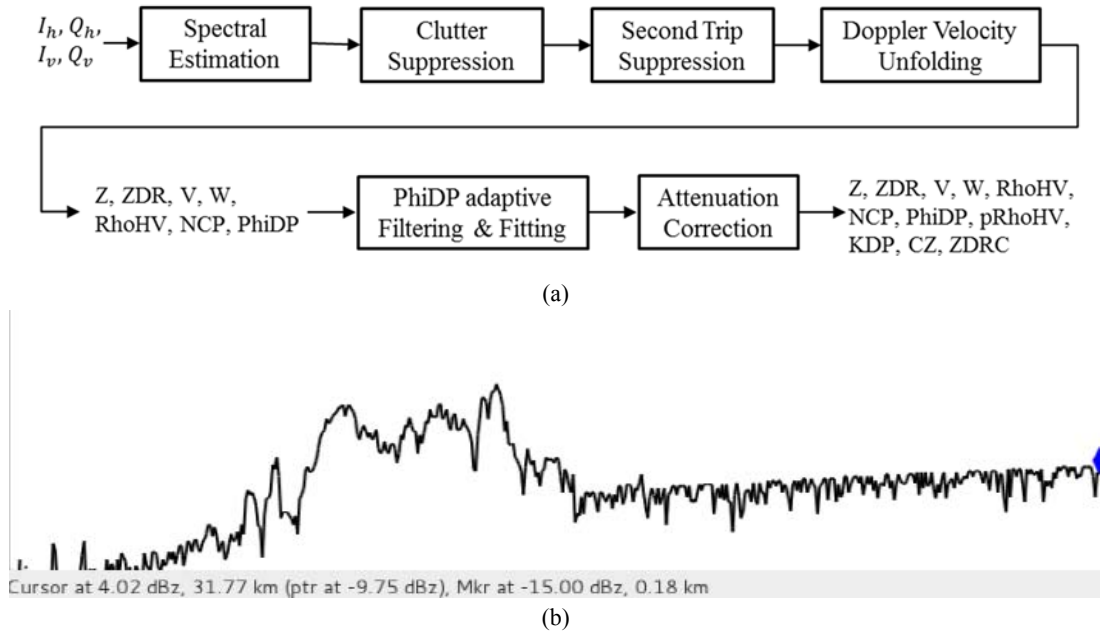


Fig. 1. Schematic diagram of radar signal processing and sample reflectivity (a) Quality control process and radar variables of dual-polarization radar, (b) Reflectivity obtained in real time from an X-band radar through the process shown in (a).

challenging in a real time radar display system. The proposed technique displays 3D radar data in real time on the GIS platform and can reveal clutter and shadowing region resulted in terrain blockage intuitively. The proposed technique maps highly accurate 3D radar data over the signal-processed 1D radar variables obtained from a dual-polarization Doppler radar. The technique displays the 3D radar data in combination with 2D and 3D GIS data in order to analyze the precipitation observation accurately. Figure 2 demonstrates the process of carrying out the proposed technique.

To display 3D radar data in real time, as shown in Figure 2, the 1D variables obtained from the radar, which is the information of each ray, is first extracted while the information of the header of the ray and of the radar variables are processed separately. For 3D displaying, the information of the header of the ray and variables used are defined in Table 1. Figure 3 shows an example of a radar beam shape model using each variable in Table 1. Figure 3(a) demonstrates the radar beam shape at the azimuthal direction (a), whereas Figure 3(b) expresses the beam shape at elevation direction (e) when the radar is observed from the side. Figure 3(c) shows an example of reflectivity profile along a ray, which is obtained in real time from a dual-polarization radar. Here, the radar beam shape is assumed to be circular at the propagating plane, and the beam width (w) and the observation radius (r) have the same values as shown in Figs. 3(a) and (b). Normalized angle values between 0 and 1 are used as the azimuth of **a** and the elevation angle of **e** to make it easy to coordinate them with various GIS coordinate systems. Range gate resolution is determined by the radar spatial resolution **h** as indicated in Table 1 and calculated as  $h=r/nGates(m)$ .

Table 1. Attribute values to be used for the 3D change of a single ray and their roles.

Attributes from ray info.	Roles	Parameters in 3D visualization	
Ray Header	Start/End Azimuth	Determination of azimuth in the 3D space	Normalized azimuth <b>a</b> = <b>[0.00~1.0]</b> of the ray object in the 3D space
	Start/End Elevation	Determination of the angle of altitude in the 3D space	Normalized angle of elevation <b>e</b> = <b>[0.00~1.0]</b> of the ray object in the 3D space
	Range	Distance from radar of 3D ray	Radar radius <b>r</b> in the 3D space
	Beam Width	Angle of the 3D ray object	Horn angle <b>w</b> of the ray object in the 3D space
	Gate Resolution	Spatial resolution of 3D ray	Spatial resolution <b>h</b> = $\frac{r}{nGates}$ (m) within radar radius <b>r</b> in the 3D space
Variable	Z, V, W, SQI, Zdr, PhiDP, CZ, KDP, RhoHV, NCP, ZDR, etc.	Radar observation variables represented in colors or as particles	Radar variable values represented in the 3D space by legend and visual threshold <b>th</b> of each variable

The proposed technique estimates the shape of the real radar beam, as shown in Figure 3, to display realistic radar data and to model the object of the 3D ray into a horn shape using the parameters in Table 1.

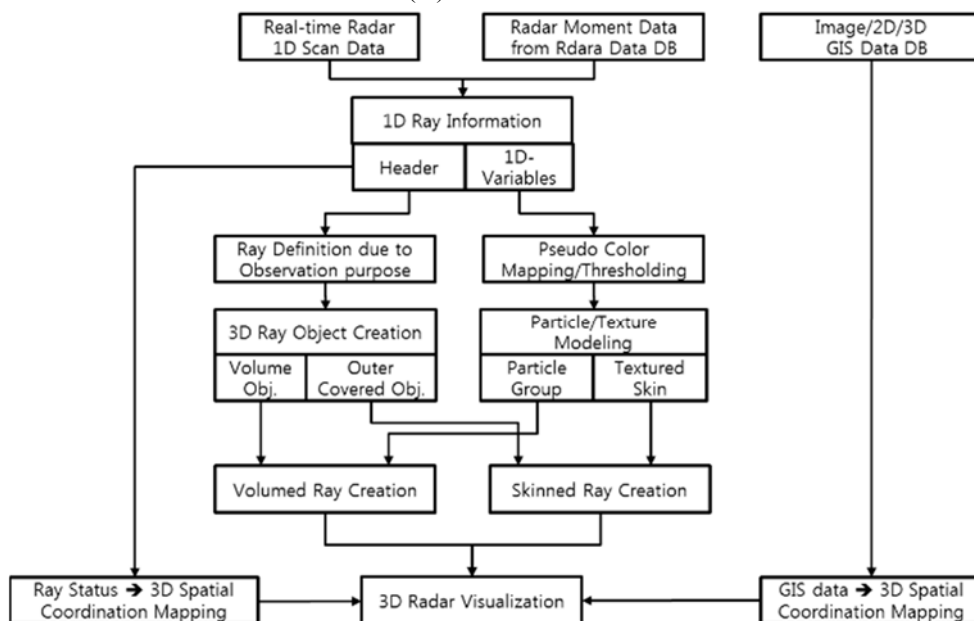


Fig. 2. Process of performing the proposed realistic radar image visualization.

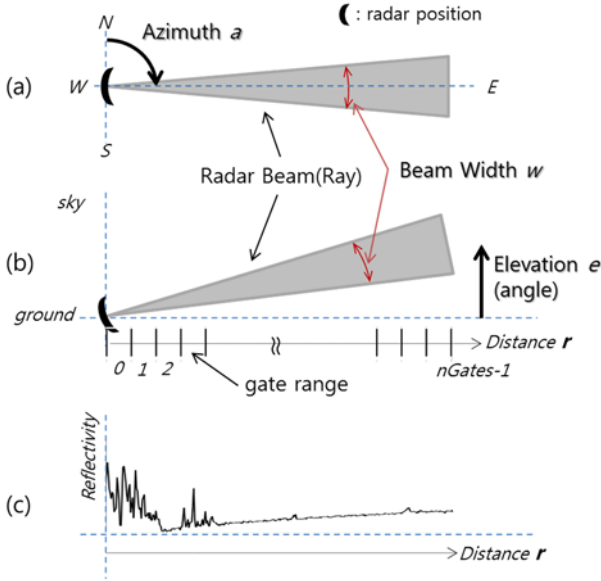
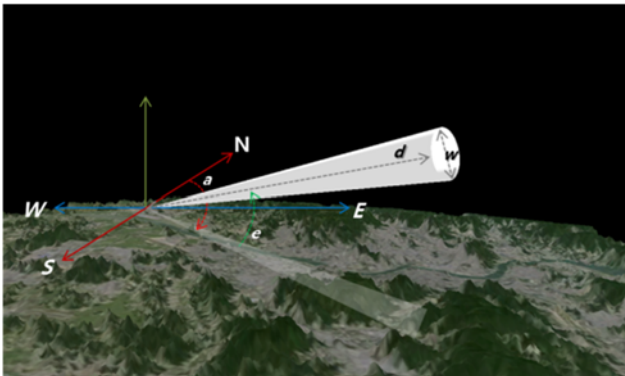
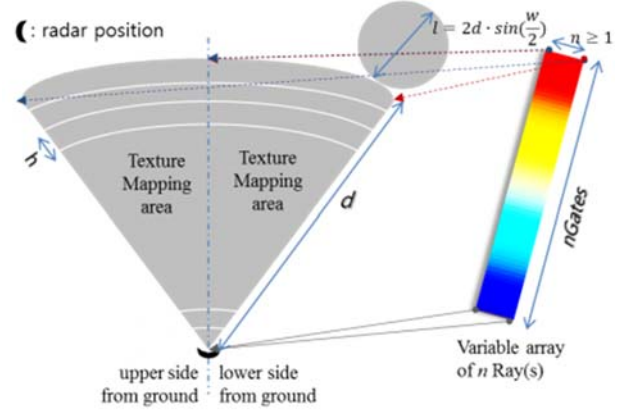


Fig. 3. The relation between each variable in Table 1 and real reflectivity patterns along a ray: (a) the shape of the radar beam on the horizontal line, (b) the shape of the radar beam on the vertical line, and (c) reflectivity from the radar.

To simplify analyzing data for an observer's purpose, the object can be formed into horns of various shapes such as plain, circular, rectangular, and hexagonal. Figure 4(a) shows the mimetic diagram of a 3D beam with circular shape using the radar variables in Table 1. Here, the object position that will be seen on GIS is calculated with the radar's coordinate position, azimuth ( $a$ ), and the elevation angle of ( $e$ ), according to the GIS coordinate system using TM (transverse Mercator) or Lat/Lon. In the proposed technique, a 2D array is formed with respect to  $n \geq 1$  numbers of rays, following which the beam object in Figure 4(a) is classified into upper and lower surfaces based on ground surface. Then, texture mapping is conducted as in Figure 4(b). Finally, radar variables are represented in the 3D beam object. Additionally, the proposed technique is designed to determine the expression method and range of 3D radar data, according to the legend and visual threshold ( $th$ ) of each radar variable.



(a)

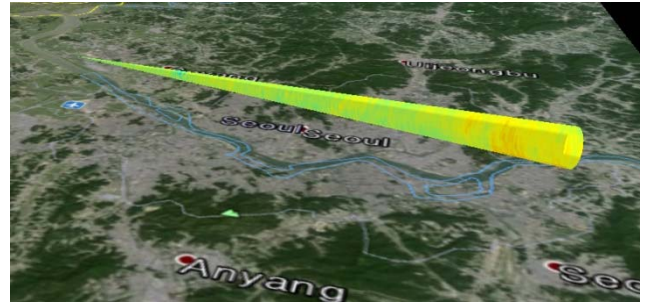


(b)

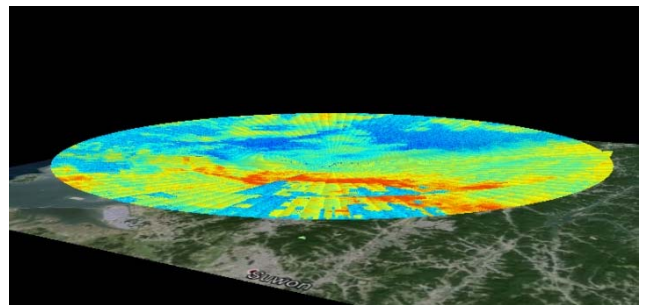
Fig. 4. An example (circular horn) of forming a 3D radar beam object using each variable in Table 1: (a) 3D object modeling in GIS, (b) radar variable texturing on 3D object.

#### IV. SIMULATION RESULT

To simulate the proposed 3D displaying technique of real-time weather radar data, data obtained from the X-band dual-polarization radar of the Korean Institute of Civil Engineering and Building Technology (KICT) and the API of the Open GL[10] 3D graphic library were used. For the GIS coordination, a 2D image map based on a precise TM coordinate system was also used. Figure 5 shows various 3D radar data displays that were constructed using the proposed technique. Figure 5(a) is an example of the 3D object formed using 8 rays and (b)-(d) indicate beam displays with plain, hexagon, and circular shape, respectively.



(a)



(b)

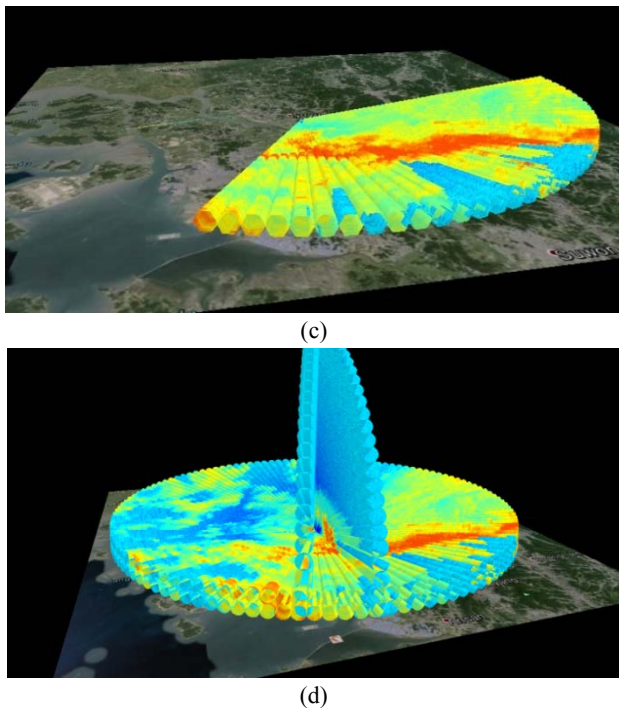


Fig. 5. Various methods of displaying the 3D radar beam in the proposed technique: (a) example of the 3D object formed using 8 rays, (b) beam display with a plain shape, (c) beam display with a hexagon shape, (d) beam display with a circular shape.

For real-time observation of massive time-series radar data in real radar observation environments, it is common to construct a dedicated optical communication network between the radar signal processing server and the monitoring system. However, since it is difficult to use the weather radar operating in the field in real time to evaluate the real-time usability of the proposed method, the simulation is performed in an emulation environment where a dedicated network is assumed. Using the previously observed radar moment data, we confirmed that 3D builds and real-time updates are performed without any delays for the transmitted rays obtained by emulating at a rate of 2 Rays/sec. for 720 ray profiles/ 360 azimuth degrees.

The proposed technique enables the weather observer to control the corresponding radar variable threshold based on the characteristics of each radar variable, making it easy to analyze the displayed data. Figure 6 shows the outcome of the threshold change in CZ (corrected reflectivity) in dBZ unit.

Target reflectivity caused by ground clutters in a quality controlled radar image is eliminated via GCF (ground clutter filtering) using Doppler velocity. By using the proposed visualization technique, we can know the GCF filtered areas intuitively from 3D expressed radar beams on the digital elevation modeled GIS map. Figure 7 shows the terrain masking influence of radar beams so that an

observer can draw a fine distinction between GCF filtered and no-echo area.

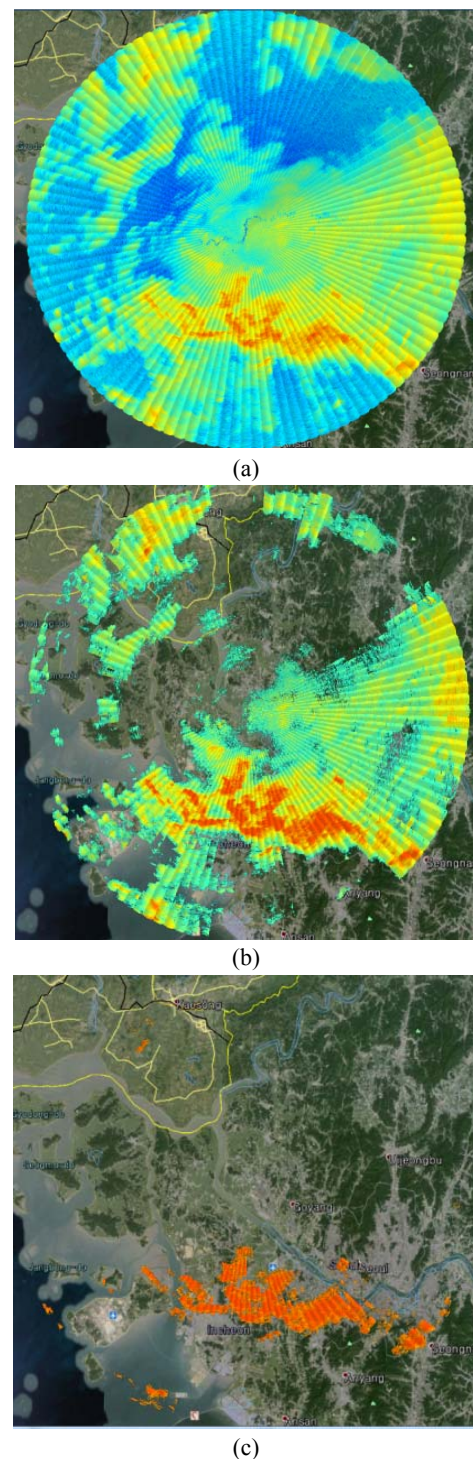


Fig. 6. 3D display outcome depending on threshold (th) change in the proposed technique: (a) th=0dB, (b) th=15dB, and (c) th=35dB.

From figure 7(a) and (b) we can possibly know that the propagations of quality controlled radar beams at low elevations were blocked by mountains. Accordingly, this technique can facilitate some post processing, such as

precipitation correction about GCF filtered areas, by observing expressed beams on the 3D GIS Map.

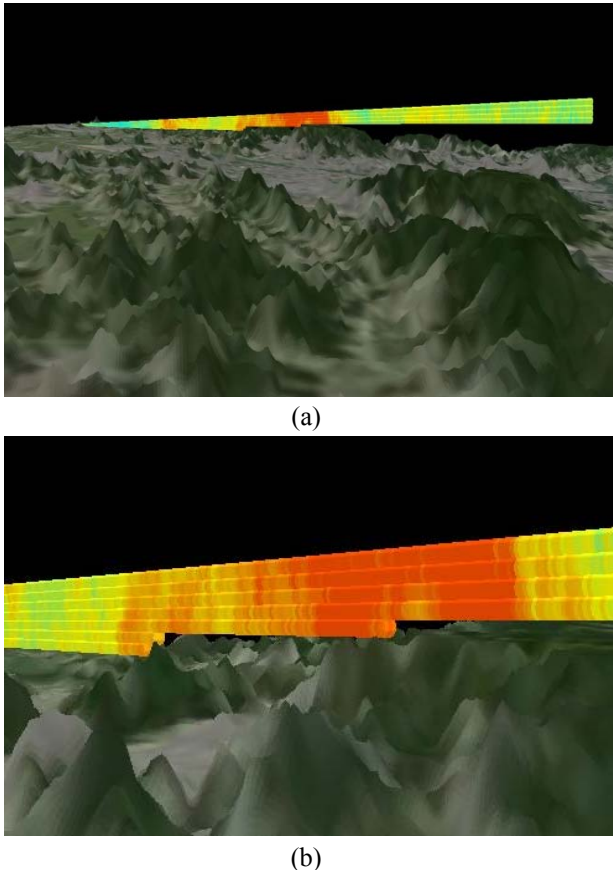


Fig. 7. Terrain masking Influence of quality controlled reflectivity via GCF based on 3D GIS Map, (a) RHI scanning radar beams, (b) partial extension of (a)...

#### IV. CONCLUSION

This paper proposes a realistic 3D weather radar data display technique with higher spatiotemporal resolution, which is based on the integration of 3D image processing and GIS interaction. This method is focused on stereoscopic visualization, while conventional radar data display methods are based on flat or two-dimensional interpretation. Furthermore, using the proposed technique, the atmospheric change at each moment can simultaneously be observed three-dimensionally at various geological locations. Simulation results indicate that 3D display of weather radar data can be performed in real time. One merit of the proposed technique is that it can provide intuitive understanding of the influence of beam blockage by topography. Through an exact matching each 3D modeled radar beam with 3D GIS map, we can find out the terrain masked areas. Accordingly, the method facilitates the precipitation correction from QPE underestimation caused by GCF. It can also be expected that more accurate short-term forecasting will be possible using stereoscopic observation of weather phenomena

changes. Furthermore, we expect that our visualization technique can help people who want to learn the radar system to understand its concept and principle.

#### Acknowledgement

This study was conducted with financial support from the MOLIT National R&D Program (Integration of Electromagnetic Wave Precipitation Gauge System and Its Performance Testing).

#### REFERENCES

- [1] V. Chandrasekar, et al., "Accomplishments, challenges and opportunities in developing network based radar systems for high-impact small-scale weather events," *2011 IEEE RadarCon (RADAR)*, Kansas City, MO, pp. 1056-1061, May 2011.
- [2] J. C. Hinton, "GIS and remote sensing integration for environmental applications," *International Journal of Geographical Information Systems*, vol. 10, no. 7, pp. 877-890, 1996.
- [3] V. Sundaram, L. Zhao, C. X. Song, B. Benes, R. Veeramacheni, and P. Kristof, "Real-time data delivery and remote visualization through multi-layer interfaces," *2008 Grid Computing Environments Workshop*, Austin, TX, pp. 1-10, 2008.
- [4] X. Zhang, and R. Srinivasan, "GIS-based spatial precipitation estimation using next generation radar and raingauge data," *Environmental Modelling & Software*, vol. 25, no. 12, pp. 1781-1788, 2010.
- [5] "J.S. Marshall Radar Observatory", <http://www.radar.mcgill.ca>, 2016.
- [6] M. R. Duncan, A. Bellon, A. Kilambi, and G. L. Austin, "PPS and PPS Jr: A distribution network for weather radar products, severe weather warnings and rainfall forecasts," *Eighth Int. Conf. on Interactive Information and Processing Systems for meteorology, oceanography and hydrology*, Atlanta, GA, Amer. Meteor. Soc., pp. 67-74, 1992.
- [7] Vaisala IRIS Datasets, "Three dimensional display for radar data Vaisala IRIS 3D View", <http://www.vaisala.com/en/defense/products/weatherradar/Pages/IRIS.aspx>, 2016.
- [8] C. N. James, S. R. Brodzik, H. Edmon, R. A. Houze, S. E. Yuter, "Radar data processing and visualization over complex terrain," *Weather and Forecasting*, Vol. 15, No. 3, pp. 327-338, 2000.
- [9] V. N, Bringi and V. Chandrasekar, *Polarimetric Doppler Weather Radar: Principles and Applications*. New York, NY: Cambridge University Press, 2001.
- [10] "OpenGL Library", <http://www.opengl.org>, 2016.

## Authors



**Bong-Joo Jang** received his B.S. and M.S. degrees in electronic engineering from Busan University of Foreign Studies, and Ph.D. degree in information security from Pukyong National University in 2002, 2004 and 2013 respectively. He visited Colorado State University in USA at 2011–2012 with visiting scholar. He is currently a Postdoctoral Research

Fellow in Korea Institute of Civil Engineering and Building Technology. His research interests include multimedia data compression and digital image/video/vector processing, and now his major interests are weather radar system, radar signal processing and weather forecasting.



**Sanghun Lim** received the Ph.D. degree in Electrical Engineering from the Colorado State University in 2006. Since then he had carried out various researches in radar meteorology and hydrology as research scientist of Colorado State University and NOAA/CIRA. Currently, he is a research fellow at Korea Institute of Civil Engineering and Building Technology and

pursuing development of advanced weather observation systems and radar remote sensing using dual-polarization radars and automotive sensors.

